Asymmetric capillary filling of non-Newtonian power law fluids

Claudio L. A. Berli & Raúl Urteaga

A 20975

Volume 17 · Number 6 · December 2014

Microfluidics and Nanofluidics

Springer

Springer

Springer

RESEARCH PAPER

Asymmetric capillary filling of non-Newtonian power law fluids

Claudio L. A. Berli · Raúl Urteaga

Abstract A theoretical analysis of the capillary-driven imbibitions of non-Newtonian fluids in conical capillaries is presented. More precisely, the consequences of the variation in the fluid viscosity with the shear rate are investigated by using the inelastic power law model. Novel fluid dynamic behaviors are predicted, notably the asymmetry of filling times measured from different ends of the conical tube. The effect is due to the anisotropy of the flow domain and takes place with simple Newtonian fluids indeed. It is quantitatively described how shear-thinning fluids increase the asymmetry, and shear-thickening fluids decrease it. Relevant applications in microfluidic rheometry are envisaged. In addition, these results are of interest in active fields of research such as passive micropumping and microflow rectification, where the geometric design of microchannels is the key to control fluidic operations.

Keywords Capillary filling · Conical capillaries · Asymmetric filling · Power law fluids · Microfluidic rheometry

1 Introduction

The phenomenon of capillary filling, which has been mathematically described almost a century ago (Lucas 1918; Washburn 1921), is now finding a number of applications in microfluidic devices (Delamarche et al. 2005; Zimmermann et al. 2007; Martinez et al. 2008; Li et al. 2011; Safavieh and Juncker 2013). In these systems, the flow rate of liquids is determined by both the wetting properties of solid/liquid interfaces and the geometry of microchannels, valves and micropumps. Thus, liquid handling is encoded in the geometric design of each component of the fluidic circuits.

Controlling the capillary-driven flow in such confinements becomes critical in the case of non-Newtonian fluids, such as blood, saliva, protein and DNA solutions, which are ubiquitous in lab-on-a-chip devices for biomedical applications. On the other hand, polymeric liquids are employed in microfabrication processes that make use of capillary action, for instance injection molding (Kim et al. 1995) and flip-chip encapsulation (Young 2011). Therefore, modeling the filling dynamics of non-Newtonian liquids is of interest to attain a better understanding of physical basis and to assist the design and manipulation of microfluidic devices. The works on the subject found in the literature are scarce; notable exceptions are the studies of capillary filling of power law (PL) fluids in rectangular microchannels (Srivastava and Burns 2006; Girardo et al. 2007) and cylindrical capillaries (Digilov 2008; Cito et al. 2012).

In this context, the objective of the present work is to discuss the capillary filling of non-Newtonian fluids in tubes with nonuniform cross section. The nonuniformity consists in a slight variation in the tube radius, whereas the inner wall is supposed to be chemically homogeneous and locally flat. It is worth noting that roughness and surface patterning influence the filling dynamics (Kusumaatmaja et al. 2008; Girardo et al. 2012); hence, these effects should be taken into account if present. More precisely, this work deals with conical capillaries with smooth surfaces, which exhibit a marked asymmetry of filling times even for

C. L. A. Berli (✉)
INTEC (UNL - CONICET), Güemes 3450,
3000 Santa Fe, Argentina
e-mail: cberli@santafe-conicet.gov.ar

R. Urteaga
IFIS-Litoral (UNL - CONICET), Santa Fe, Argentina

simple Newtonian fluids (Urteaga et al. 2013). Focus is made on the effect of the variation in the fluid viscosity η with the shear rate $\dot{\gamma}$, independently of elasticity. The asymmetric filling is of special interest for the design of fluidic diodes that facilitate the transport of liquids in one direction only (Chen et al. 2012; Feng and Rothstein 2013). Also, relevant applications in microfluidic rheometry are envisaged.

The paper is organized as follows: next section presents the theoretical basis and the equations to describe capillary flow of PL fluids in conical channels. Then, the results are presented and discussed in comparison with simple Newtonian fluids. Finally, the main conclusions are outlined.

2 Theoretical modeling

The analysis here is restricted to the domain of continuum fluid mechanics, and thus, potential effects associated with the discreteness of the fluid microstructure are disregarded (see for instance Holloway et al. 2011). The approximation is valid when the average size of particles/macromolecules constituting the complex fluid is small comparing to the capillary radius. To predict the capillary filling dynamics, first step consists in the selection of a constitutive model for the fluid viscosity. A simple function $\eta(\dot{\gamma})$ that reasonably describes the non-Newtonian viscosity of inelastic fluids is the PL model of Oswald–de Waele, $\eta(\dot{\gamma}) = k\,\dot{\gamma}^{n-1}$, where n is the flow behavior index and k is the consistency parameter (de Waele 1923; Ostwald 1925). Values of $n < 1$ represent shear-thinning or pseudoplastic fluids, while $n > 1$ represent shear-thickening or dilatants fluids. When $n = 1$, the Newton model is recovered, k being equal to the viscosity coefficient μ.

The flow rate Q of PL fluids in capillaries of circular cross section is readily obtained for steady state, fully developed, and unidirectional flows (Bird et al. 1977):

$$Q = \frac{\pi R^3}{(3 + 1/n)} \left(\frac{R}{2k} \left| \frac{dp}{dx} \right| \right)^{1/n}, \tag{1}$$

where R is the tube radius and dp/dx is the pressure gradient along the axial direction x. For slight variations in the tube cross section, one may introduce $R(x)$ as the axially dependent channel radius. As Q is constant for incompressible fluids, Eq. 1 can be integrated to calculate the pressure drop Δp across the filled section of the tube,

$$\left(\frac{(3 + 1/n)Q}{\pi} \right)^n 2k \int_0^x \frac{dx'}{R(x')^{3n+1}} = \Delta p. \tag{2}$$

If gravity effects are disregarded, the right-hand side of Eq. 2 corresponds to Laplace pressure, $\Delta p = 2\sigma \cos\theta/R$,

where σ is the surface tension of the fluid, and θ is the contact angle of the meniscus at the liquid–gas interface. Our analysis involves the fluid dynamic regime where the filling kinematics is controlled by viscous dissipation (Fries and Dreyer 2008). Therefore, the axial velocity of the meniscus can be written $dx/dt = Q/(\pi R^2)$, and Eq. 2 is converted into the following expression,

$$\left(\frac{dx}{dt} \right)^n = \frac{c}{(3 + 1/n)^n R(x)^{2n+1} \int_0^x R(x')^{-(3n+1)} dx'}, \tag{3}$$

where $c = \sigma \cos\theta/k$. Equation 3 governs the filling dynamics of PL fluids in tubes of nonuniform cross section. As gravity is not included here, the results of Eq. 3 apply to horizontal capillaries, or in systems where gravitational forces are relatively small (Das and Mitra 2013). The reader is referred to the work of Digilov (2008) for a discussion of capillary rise of PL fluids in cylindrical tubes.

In the trivial case of tubes with uniform radius, the integration of Eq. 3 yields,

$$x^{(1+n)/n} = \frac{(n + 1)Rc^{1/n}t}{(3n + 1)}, \tag{4}$$

in agreement with previous analysis of PL fluids in cylindrical capillaries (Girardo et al. 2007; Cito et al. 2012). In particular, if $n = 1$, Eq. 4 results $x^2 = Rct/2$, which is the classical Lucas–Washburn equation for simple fluids (Lucas 1918; Washburn 1921). Also from Eq. 4, the characteristic filling time for PL fluids is defined as the time at which the meniscus reaches the tube length L,

$$t_{F,n} = \frac{(3n + 1)L^{1/n+1}}{(n + 1)Rc^{1/n}}. \tag{5}$$

In what follows, we use Eq. 3 to derive the kinematics of fluid imbibition in nonuniform capillaries. Let us consider axisymmetric conical capillaries with the smallest radius R_0 at the inlet ($x = 0$) and the largest radius R_L at the outlet ($x = L$). The cone angle $\alpha \approx (R_L - R_0)/L$ must be very small, so that the assumption of unidirectional flow is accurate. Thus, the radius changes along the channel as $R(x) = R_0 + \alpha x$. Introducing $\widehat{R} = R(x)/R_0$ and $d\widehat{R} = \alpha dx/R_0$ into Eq. 3, integrating the time derivative yields

$$\int_1^{1+\alpha x/R_0} \left(\widehat{R}^{2n+1} - \widehat{R}^{1-n} \right)^{1/n} d\widehat{R} = \frac{(3n\alpha c/R_0)^{1/n}\alpha t}{(3 + 1/n)}. \tag{6a}$$

On the other hand, if the fluid enters through the largest end and flows toward the smallest end, the channel radius varies in the flow direction as $R(x) = R_L - \alpha x$. Introducing $\breve{R} = R(x)/R_L$ and $d\breve{R} = -\alpha dx/R_L$ into Eq. 3, integrating the time derivative results

$$-\int_{1}^{1-\alpha x/R_L} \left(-\breve{R}^{2n+1} + \breve{R}^{1-n}\right)^{1/n} d\breve{R} = \frac{(3n\alpha c/R_L)^{1/n}\alpha t}{(3+1/n)}.$$

(6b)

Equation 6a, 6b cannot be solved analytically for arbitrary values of n. Useful exceptions are the cases of $n = 1$ and $n = 1/2$. We outline these solutions below to be used later in the analysis of the filling dynamics of shear-thinning fluids, in comparison with Newtonian fluids. In fact, solving Eq. 6a, 6b for $n = 1$ leads to the following expressions for the capillary filling of opening and closing cones, respectively,

$$\frac{1}{6}\beta^2\bar{x}^4 + \frac{2}{3}\beta\bar{x}^3 + \bar{x}^2 = \frac{t}{t_{F,n}(R_0)},$$

(7a)

$$\frac{1}{6}\left(\frac{\beta}{1+\beta}\right)^2\bar{x}^4 - \frac{2}{3}\left(\frac{\beta}{1+\beta}\right)\bar{x}^3 + \bar{x}^2 = \frac{t}{t_{F,n}(R_L)},$$

(7b)

where $\bar{x} = x/L$ and $\beta = (R_L - R_0)/R_0$. Also in these equations, $t_{F,n}(R_0)$ and $t_{F,n}(R_L)$ represent the filling times of capillaries with uniform radius R_0 and R_L, respectively (Eq. 5, $n = 1$). In addition, solving Eq. 6a, 6b for $n = 1/2$ yields the following expressions for opening and closing cones, respectively,

$$\frac{4}{15}(1+\beta\bar{x})^5 - \frac{16}{21}(1+\beta\bar{x})^{7/2} + \frac{2}{3}(1+\beta\bar{x})^2 - \frac{6}{35} = \frac{\beta^3 t}{t_{F,n}(R_0)},$$

(8a)

$$-\frac{4}{15}\left(1-\frac{\beta\bar{x}}{\beta+1}\right)^5 + \frac{16}{21}\left(1-\frac{\beta\bar{x}}{\beta+1}\right)^{7/2}$$
$$-\frac{2}{3}\left(1-\frac{\beta\bar{x}}{\beta+1}\right)^2 + \frac{6}{35} = \left(\frac{\beta}{\beta+1}\right)^3\frac{t}{t_{F,n}(R_L)},$$

(8b)

where the corresponding filling times $t_{F,n}$ now involve $n = 1/2$. Equation 8a, 8b may have practical interest as well, taking into account that shear-thinning behaviors with flow index $n \sim 1/2$ are typical in colloids and polymer solutions.

3 Results and discussions

3.1 PL fluids in cylindrical capillaries

Firstly, the capillary filling of PL fluids in cylindrical tubes is revised, in order to analyze the impact of the shear rate dependence of fluid viscosity, independently of geometric effects. The prediction of Eq. 4 is illustrated in Fig. 1. It is relevant to point out that the filling response of PL fluids in uniform capillaries has been experimentally validated in previous works: Girardo et al. (2007) used phenyl glycidyl
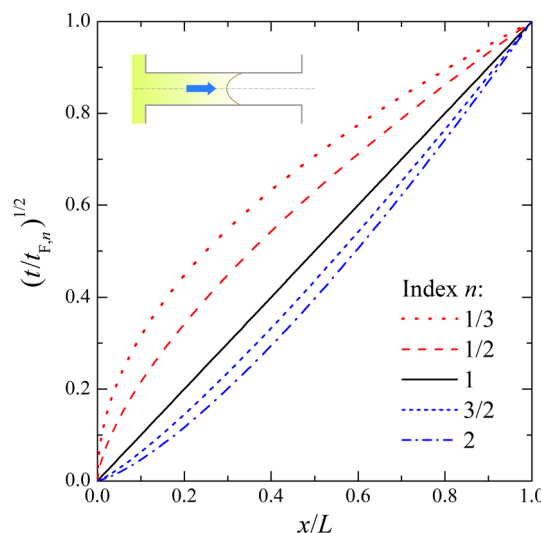
Fig. 1 Square root of the relative time as a function of the relative meniscus position, according to Eq. 4, for different values of the flow index n. Calculations are thus independent of R, L, and c

ether ($n = 0.41$) in rectangular microchannels, and Digilov (2008) used aqueous solutions of carboxymethyl cellulose ($n = 0.73$–0.78) in cylindrical capillaries.

A relevant feature in Fig. 1 is the variation in the slope of the curve x versus $t^{1/2}$ during the filling process, as compared to the case of Newtonian fluids. To better understand these results, one needs to consider the shear rate at channel walls, which is $\dot{\gamma}_w = Q(3 + 1/n)/(\pi R^3)$ (Bird et al. 1977). Introducing $Q = \pi R^2 dx/dt$, the above expression results $\dot{\gamma}_w = (c/x)^{1/n}$ (see also Girardo et al. 2007; Digilov 2008). The shear rate decreases with x, irrespective of the flow index n, because the fluid velocity always decreases during capillary imbibition. For non-Newtonian fluids, however, this means a variation in fluid viscosity in time. In fact, considering the above expression of $\dot{\gamma}_w$, the apparent viscosity results $\eta \approx k(c/x)^{1-1/n}$. Therefore, while the fluid advances into the capillary, the apparent viscosity varies as $x^{1/n-1}$ and accordingly as $t^{(1-n)/(1+n)}$. Thus, the fluid viscosity increases in time for $n < 1$ and decreases for $n > 1$, which explains the variation in curve slopes in Fig. 1. Of course, the viscosity is constant for $n = 1$ and Lucas–Washburn regime is recovered (straight line x vs. $t^{1/2}$).

It is worth mentioning that the time variation in the viscosity discussed here is just a consequence of the variation in $\dot{\gamma}$ with x, while the meniscus advances into the capillary in pseudo-steady-state. Actually, the PL model cannot describe time-dependent responses nor viscoelastic phenomena. These effects take relevance when $\dot{\gamma}^{-1}$ is on the order of the characteristic relaxation time of the fluid, and may arise at the early stages of the filling process, where $\dot{\gamma}$ virtually diverges.
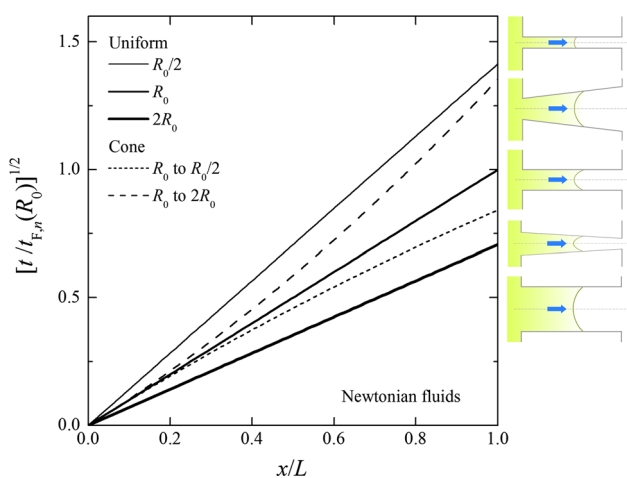
Another drawback of the PL model to describe capillary-driven flow is the loss of reliability at the beginning of the imbibition, because the extremely large shear rates developed in capillaries may induce artificial viscosity values. For example, if one considers a polymer solution that satisfies the PL model for, say, $1 < \dot{\gamma} < 10^3 \text{ s}^{-1}$, at $x \ll L$ the model could predict fluid viscosities lower than that of the solvent, which is evidently unphysical. A more realistic model including a high-shear rate-limiting viscosity must be included to better describe the fluid imbibition at short distances/times, for instance the Carreau model (Bird et al. 1977). In this case, however, no explicit expression of dx/dt for capillary imbibitions could be obtained.

Another relevant aspect related to high shear rates in micro- and nanochannels is the violation of the no-slip condition at channel walls (Lauga et al. 2007), which is implicit in the derivation of Eq. 1. Furthermore, in complex fluids, an apparent hydrodynamic slip may also take place due to depletion of particles/polymer molecules at the solid liquid interface (Nghe et al. 2011; Berli 2013). For these cases, incorporating the typical slip condition (fluid velocity at the wall is not zero but a value proportional to $\dot{\gamma}_w$) do not modify the PL scaling of Q with Δp; hence, the final $x(t)$ functionality is not significantly changed.

3.2 Newtonian fluids in conical capillaries

Now, we discuss the filling dynamics of simple fluids in conical capillaries, in order to analyze the influence of the geometry independently of non-Newtonian effects. The predictions of Eq. 7a, 7b are illustrated in Fig. 2. In capillaries of uniform cross section, the filling time is inversely proportional to the tube radius, as seen in Eq. (5). In a conical capillary, however, as the radius diverges from R_0 to $2R_0$ (in the flow direction), the filling time becomes larger than that corresponding to a cylinder with radius $R < R_0$. In other words, if one regards the cone as an equivalent cylinder, the equivalent cylinder radius is not between R_0 and $2R_0$, but it is smaller than R_0. And the opposite happens in converging capillaries. This rather counterintuitive behavior is due to the fact that, as the meniscus advances into the conical geometry, the viscous force varies as $R(x)^{-2}$ while capillary force varies as $R(x)^{-1}$. Further details on this feature are given in a previous work (Urteaga et al. 2013).

The drawings in Fig. 2, as well as those in Figs. 3 and 4 below, are out of scale. One should remind that the analysis here is valid for fully developed, unidirectional flows, which requires capillaries with both very large aspect ratios ($R_0 \ll L$) and very small cone angles ($\alpha \ll 1$).

3.3 PL fluids in conical capillaries

The filling dynamics of shear-thinning fluids in conical capillaries is illustrated in Fig. 3, according to Eq. 8a, 8b. The geometric effect discussed above is now emphasized by the $\dot{\gamma}$-dependence of the viscosity, and predictions are quite more striking: the filling time of a conical capillary that opens from R_0 to $2R_0$ is larger than that corresponding to a cylinder with radius $R < R_0/2$. To rationalize these results, one has to take into account that, in a diverging capillary, there is an additional decrease in the shear rate along the tube due to the gradual enlargement of the flow
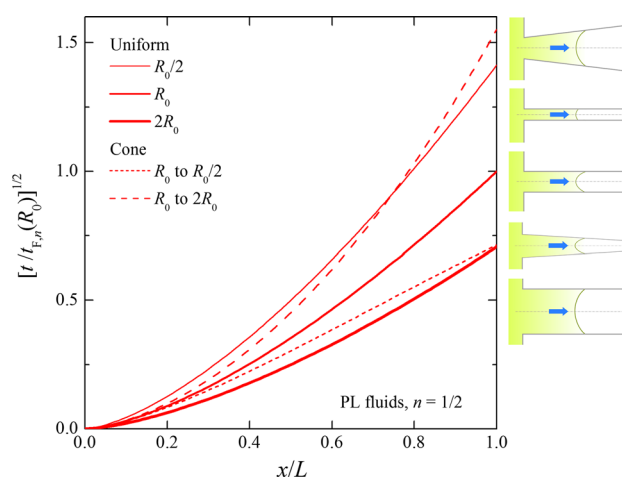

Fig. 2 Square root of the relative time as a function of the relative meniscus position for Newtonian fluids in conical tubes (Eq. 7a, 7b, $\beta = 1$), in comparison with cylindrical capillaries (Eq. 4, $n = 1$). The drawings on the right are, from *bottom* to *top*, in the sequence of the filling times of the corresponding curves

Fig. 3 Square root of the relative time as a function of the relative meniscus position for PL fluids with $n = 1/2$ in conical tubes (Eq. 8a, 8b, $\beta = 1$), in comparison with cylindrical capillaries (Eq. 4, $n = 1/2$). The drawings on the right are, from *bottom* to *top*, in the sequence of the filling times of the corresponding curves

domain. This variation in $\dot{\gamma}$ with x induces a relative increase in the fluid viscosity, hence the filling time, in comparison with a Newtonian fluid in the same cone. The opposite effect takes place in the case of converging channels: as seen in Fig. 3, the meniscus velocity firstly decreases and then increases in the second half of the tube. This is because of the relative variation in fluid viscosity, as $\dot{\gamma}$ decreases slowly when the flow domain shrinks.

3.4 Asymmetric capillary filling

The overall result is a strong asymmetry of the filling times, when measured from different sides of the same conical capillary. In fact, taking the ratio of Eq. 6a, 6b with $x = L$ (complete filling) yields the following expression,

$$\frac{t_O}{t_C} = \left(\frac{R_L}{R_0}\right)^{1/n} \frac{\int_1^{R_L/R_0} \left(\widehat{R}^{2n-1} - \widehat{R}^{1-n}\right)^{1/n} d\widehat{R}}{\int_{R_0/R_L}^1 \left(\widecheck{R}^{1-n} - \widecheck{R}^{2n+1}\right)^{1/n} d\widecheck{R}}, \tag{9}$$

where the left-hand side is the ratio between the time required to fill the capillary in the opening cone direction, t_O, and that in the closing cone direction, t_C. Equation 9 indicates that t_O/t_C is completely defined by the ratio R_L/R_0 and the flow index n. The filling time asymmetry of conical capillaries is illustrated in Fig. 4, after numerical solution of Eq. 9.

It is worth noting that the asymmetric filling is in principle due to the nonuniform character of the capillary, as evidenced by the curve for simple fluids ($n = 1$). Figure 4 shows how shear-dependent viscosities modify the asymmetry: shear-thinning fluids enhance the effect, while shear-thickening fluids reduce it. In any case, Fig. 4 exhibits the diodic character of the capillary-driven flow in conical channels, which is of great interest to handle passive transport in microfluidics.

A straightforward analysis of curves in Fig. 4 reveals a power relationship between t_O/t_C and R_0/R_L, with a power exponent $f(n)$ that depends on n only. In fact, for R_L/R_0 around 1 (more precisely, in the range plotted), one may accurately write,

$$\frac{t_O}{t_C} = \left(\frac{R_L}{R_0}\right)^{f(n)}. \tag{10}$$

Besides, we found that the function $f(n) = 7/3 + (1/n - 1)$ represents reasonably well the curves of Fig. 4: the error is less than 3 % for flow indexes in the range $1/2 \leq n \leq 3/2$. The fact that the Newtonian curve satisfies $t_O/t_C \approx (R_0/R_L)^{7/3}$ had been demonstrated by theory and experiments in our previous work (Urteaga et al. 2013).

These last results open the possibility of new applications in the field of microfluidic rheometry: measuring t_O and t_C in a conical capillary would constitute a simple and reliable method to find the flow index n of a given fluid, irrespective of other properties like viscosity and surface tension, and using a small droplet of sample. Furthermore, the ratio R_L/R_0 of the cone may be estimated by a similar measurement with any Newtonian fluid (calibration).

4 Concluding remarks

We have theoretically investigated the capillary-driven imbibition of conical capillaries with inelastic non-Newtonian fluids. Even if the simple constitutive model used has several limitations, it allows one to figure out the influence of viscosity variations on the capillary filling dynamics. Remarkable fluid dynamic behaviors were quantitatively predicted, notably the asymmetry of filling times. Apart from the theoretical aspects in microfluidics of complex fluids, these novel results open new potential applications in active fields of research such as passive micropumping and microflow rectification, where the geometric design of microchannels is crucial to control fluidic operations. Further, the application of these predictions to design simple microfluidic rheometers is currently under research in our laboratory. It is worth to add that microfluidic systems microfabricated through the standard processes involve microchannels with trapezoidal cross sections, where sharp corners pose several troubles to the mathematical description of capillary-driven transport. In any case, provided one can handle these difficulties in modeling, our calculations still apply to lab-on-a-chip devices.
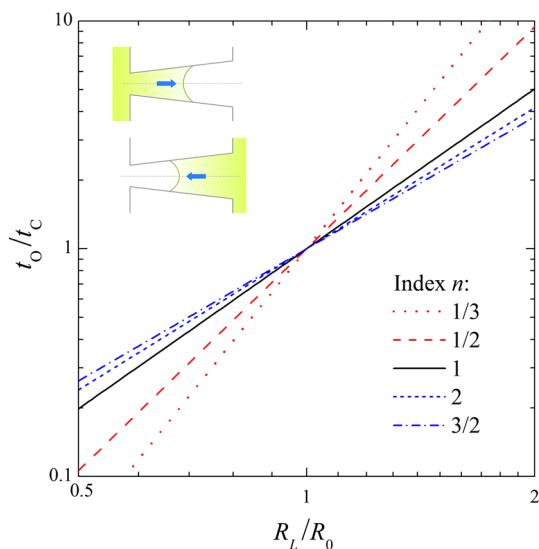
Fig. 4 Ratio of the filling times in the opening and closing cone directions, as a function of the ratio between the smallest and the largest cone radius, for different values of n, according to Eq. 9

References

Berli CLA (2013) The apparent hydrodynamic slip of polymer solutions and its implications in electrokinetics. Electrophoresis 34:622–630

Bird RB, Armstrog R, Hassager O (1977) Dynamics of polymeric liquids, vol I. Wiley, New York

Chen H, Cogswell J, Anagnostopoulosa C, Faghri M (2012) A fluidic diode, valves, and a sequential-loading circuit fabricated on layered paper. Lab Chip 12:2909–2913

Cito S, Ahn Y-C, Pallares J, Martinez Duarte R, Chen Z, Madou M, Katakis I (2012) Visualization and measurement of capillary-driven blood flow using spectral domain optical coherence tomography. Microfluid Nanofluid 13:227–237

Das S, Mitra SK (2013) Different regimes in vertical capillary filling. Phys Rev E 87:063005

de Waele A (1923) Viscometry and plastometry. J Oil Colour Chem Assoc 6:33–69

Delamarche E, Juncker D, Schmid H (2005) Microfluidics for processing surfaces and miniaturizing biological assays. Adv Mater 17:2911–2933

Digilov RM (2008) Capillary rise of a non-Newtonian power law liquid: impact of the fluid rheology and dynamic contact angle. Langmuir 24:13663–13667

Feng J, Rothstein JP (2013) One-way wicking in open micro-channels controlled by channel topography. J Colloid Interface Sci 404:169–178

Fries N, Dreyer M (2008) The transition from inertial to viscous flow in capillary rise. J Colloid Interface Sci 327:125–128

Girardo S, Cingolani R, Pisignano D (2007) Microfluidic rheology of non-Newtonian liquids. Anal Chem 79:5856–5861

Girardo S, Palpacelli S, De Maio A, Cingolani R, Succi S, Pisignano D (2012) Interplay between shape and roughness in early-stage microcapillary imbibition. Langmuir 28:2596–2603

Holloway W, Aristoff JM, Stone HA (2011) Imbibition of concentrated suspensions in capillaries. Phys Fluids 23:081701

Kim E, Sia Y, Whitesides GM (1995) Polymer microstructures formed by moulding in capillaries. Nature 376:581–584

Kusumaatmaja H, Pooley CM, Girardo S, Pisignano D, Yeomans JM (2008) Capillary filling in patterned channels. Phys Rev E 77:067301

Lauga E, Brenner MP, Stone HA (2007) Microfluidics: the no-slip boundary condition. In: Tropea C, Yarin A, Foss J (eds) Handbook of experimental fluid dynamics. Springer, New York, pp 1219–1240

Li JM, Liu C, Zhang KP, Ke X, Xu Z, Li CY, Wang LD (2011) A micropump based on water potential difference in plants. Microfluid Nanofluid 11:717–724

Lucas R (1918) Ueber das zeitgesetz des kapillaren aufstiegs von flussigkeiten. Kolloid Z 23:15–22

Martinez AW, Phillips ST, Whitesides GM (2008) Three-dimensional microfluidic devices fabricated in layered paper and tape. PNAS 105:19606–19611

Nghe P, Terriac E, Schneider M, Li ZZ, Cloitre M, Abecassis B, Tabeling P (2011) Microfluidics and complex fluids. Lab Chip 11:788–797

Ostwald W (1925) Ueber die geschwindigkeitsfunktion der viskositat disperser systeme. Kolloid Z 36:99–117

Safavieh R, Juncker D (2013) Capillarics: pre-programmed, self-powered microfluidic circuits built from capillary elements. Lab Chip (in press). doi:10.1039/C3LC50691F

Srivastava N, Burns MA (2006) Analysis of non-Newtonian liquids using a microfluidic capillary viscometer. Anal Chem 78:1690–1696

Urteaga R, Acquaroli LN, Koropecki RR, Santos A, Alba M, Pallares J, Marsal LF, Berli CLA (2013) Optofluidic characterization of nanoporous membranes. Langmuir 29:2784–2789

Washburn EW (1921) The dynamics of capillary flow. Phys Rev 17:273–283

Young WB (2011) Effect on filling time for a non-Newtonian flow during the underfilling of a flip chip. IEEE Trans Comp Packag Technol 1:1048–1053

Zimmermann M, Schmid H, Hunziker P, Delamarche E (2007) Capillary pumps for autonomous capillary systems. Lab Chip 7:119–125